

The Parametric Stability of Elastic Columns Under Different Types of Dynamic Loadings

Abdullah Dhayea Assi[†], Qasim M. Azpen[†], Salman Hussien Omran[‡]

[†]Institute of Technology-Baghdad, Middle Technical University, Iraq- Baghdad.

[‡]Ministry of Higher Education & Scientific Research, Iraq- Baghdad.

*Corresponding Author Email: drabdullah_dhayea@mtu.edu.iq

ABSTRACT: This paper is concerned with the investigation of the parametric stability of simply of supported elastic columns subjected to different types of pulsating axial dynamic loadings. The governing equation of the problem is reduced to a time-domain function by applying Galerkin method instability. These regions of this system are determined using the procedure proposed by Boletin. The primary and secondary parameter instability regions of the system subjected to rectangular and triangular periodic forces. The results have been analyses and compared with the results that obtained for a sinusoidal periodic force. Further, with increasing the added value of the (μ^2), the secondary instability zone expands and the lower border of the primary region shifts to the top and there were no tangible effects on the boundaries of the instability areas when adding ($P_6 \cos 6\theta t$, $P_5 \cos 5\theta t$ etc.) to the initial dynamic force ($P_0 + P_1 \cos \theta t$).

KEYWORDS: parametric stability, elastic columns, dynamic loadings; sinusoidal periodic forces.

INTRODUCTION

The stability issue of columns that subject to periodic loads has expanded during the past few years. Under special circumstances, it has been known that the usual forced response will become instability dynamically which leading to violent vibrations which are called parametric vibration like rotating machinery. A group researcher provided an extensive discussion of studies on this topic [1]. In other study, researchers have discussed these issues with their classification. Using the Finite Difference method [2]. Some researcher's lessons stabilize columns that are tightly secured by fixed ends, as well as simple-textures [3]. In another study, type of instability called (Combination Resonance) was discussed for four types of stabilization cases for both ends of the columns [4]. The instances of instability of Tapered columns with simply installed from both ends were studied theoretically and practically (where they found no effect the slope factor at the boundary of the instability areas compared to the regular columns [5,6]. Theoretical studies were also conducted on the effect of Pre-Twisting Angle on the instability of the flexible columns of different types of fixing the ends [7]. As for Ramu, in addition to the primary and secondary instability areas, other areas of instability called (Combination Resonance) were found equal to or more dangerous than the primary and secondary instability areas [8]. The previous studies in the field of educational stability are related to a special type of periodic force, which is the axial sinusoid type ($P_0 + p_1 \cos \theta t$). While this work aims to study the effect of a general periodic axial force such as a force with a rectangular or a triangular wave on the borders of other areas of instability of the gravity of these two regions in practice.

MATHEMATICAL ANALYSIS

The Equation of the Transverse Movement of the Column

The column is a regular and has a transverse body, Figure 1 and using Euler theory to discuss the spontaneous response of the column, where shear distortion and rotational inertia are negligible [9]. In addition, the effect of longitudinal inertia and initial curvature are imposed in small quantities, as long as the analysis is related to lower areas of instability[10-9] . Finally, the analysis below does not include the damping, so the equation for movement will be [2].

$$EI \frac{d^4 y}{dx^4} + P(t) \frac{d^2 y}{dx^2} + \rho A \frac{d^2 y}{dt^2} = 0 \dots \dots (1)$$

Where EI is the *Flexural Stiffness* of the column, y is the Transverse displacement of the column, x is the Longitudinal coordinate toward the axis of the column, t is the time, ρA is the unit mass of the column and $P(t)$ is the rotating axial force.

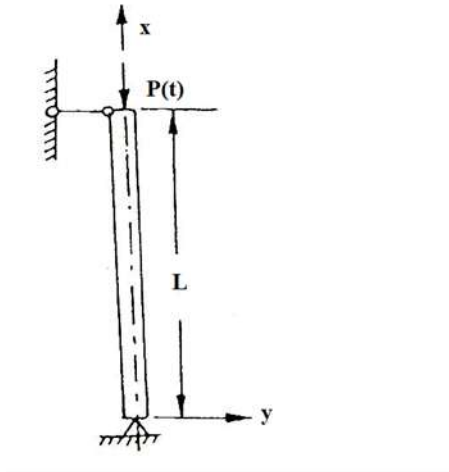


Figure 1. Column Coordinates

The rotating force $P(t)$ can be written as:

$$P(t) = \sum_{i=0}^{\omega} P_i \cos i \theta t$$

p_i is the *Fourier Series Coefficients* corresponding to the type of force $P(t)$, so equation (1) will be as follow:

$$EI \frac{\partial^4 y}{\partial x^4} + \sum_{i=0}^{\omega} P_i \cos i \theta t \frac{\partial^2 y}{\partial x^2} + pA \frac{\partial^2 y}{\partial t^2} = 0 \dots\dots\dots(2)$$

The solution to equation (2) can be as below [10]:

$$y(x, t) = f(t) \sin \frac{\pi x}{L} \dots\dots\dots(3)$$

Where $f(t)$ is the vibration amplitude in the first layout, time-dependent column format. By substituting (3) in (2) and using Galerkin variations for the column with both ends. Thus, the non-dimensional equation will be reproduced as follows:

$$\ddot{f} + \Omega^2 \left(1 - 2 \sum_{i=0}^{\omega} \mu_i \cos i \theta t \right) f = 0, \quad \ddot{f} = \frac{d^2 f}{dt^2} \dots\dots\dots(4)$$

Where Ω is the natural frequency of the column under the P_i static load, and μ_i is the excitation coefficient.

$$\mu_i = \frac{P_i}{2(P_e - P_o)}, \quad \Omega = \left(\frac{\pi}{L} \right)^2 \sqrt{\frac{EI}{\rho A} \left(1 - \frac{P_o}{P_e} \right)}$$

p_e is the Euler buckling load.

Finding Areas of the Parametric Instability

A group researchers explain that the areas with an unbounded solution of the equation (4) are separated from the regions with a restricted solution by periodic solutions with T and $2T$ periods where [2]. In other words, two solutions with two similar periods have limited the zone of instability and two solutions with two different periods surround a zone of stability. The areas confined to two solutions that have a $2T$ period are the areas of instability, as they are for the primary instability areas, while the secondary areas of instability are confined to two solutions with a period of T , and on this basis the primary instability areas:

$$f(t) = \sum_{i=1,2,3}^{\omega} \left(a_j * \sin \frac{j \theta t}{2} + b_j \cos \frac{j \theta t}{2} \right) \dots\dots\dots(5)$$

$$f(t) = \sum_{j=0,2,4}^{\infty} \left(a_j \sin \frac{j\theta t}{2} + b_j \cos \frac{j\theta t}{2} \right) \dots \dots (6)$$

Substitute Eqs. 5 and 6 in Eq. 4 to get the true solution (non-trivial) for the constructed equations. So, the following limited solution will govern the boundaries of the primary instability zones. All solutions were remedied by MATLAB:

$$\begin{vmatrix} 1 + \mu_1 - \left(\frac{\theta}{2\pi}\right)^2 & -(\mu_1 \mp \mu_2) & -(\mu_2 \mp \mu_3) & -(\mu_3 \mp \mu_4) \\ -(\mu_1 \mp \mu_2) & 1 \mp \mu_3 - \left(\frac{3\theta}{2\pi}\right) & -(\mu_1 \mp \mu_4) & -(\mu_2 \mp \mu_5) \\ -(\mu_2 \mp \mu_3) & -(\mu_1 \mp \mu_4) & 1 \mp \mu_5 - \left(\frac{5\theta}{2\Omega}\right) & -(\mu_1 \mp \mu_6) \\ -(\mu_3 \mp \mu_4) & -(\mu_2 \mp \mu_5) & -(\mu_1 \mp \mu_6) & 1 \mp \mu_7 - \left(\frac{7\theta}{2\pi}\right) \\ -(\mu_4 \mp \mu_5) & -(\mu_3 \mp \mu_6) & -(\mu_2 \mp \mu_7) & -\left(\mu_1 \mp \mu_8\right) \end{vmatrix} = 0 \dots (7)$$

The following limits lead to obtain the boundaries of the secondary instability areas:

$$\begin{vmatrix} 1 + \mu_2 - \left(\frac{\theta}{\pi}\right) & -(\mu_1 - \mu_3) & -(\mu_2 - \mu_4) & -(\mu_3 - \mu_5) \\ -(\mu_1 - \mu_3) & 1 + \mu_4 - \left(\frac{2\theta}{\Omega}\right) & -(\mu_1 - \mu_5) & -(\mu_2 - \mu_6) \\ -(\mu_2 - \mu_4) & -(\mu_1 - \mu_5) & 1 + \mu_6 - \left(\frac{3\theta}{\Omega}\right) & -(\mu_1 - \mu_7) \\ -(\mu_2 - \mu_4) & -(\mu_2 - \mu_6) & -(\mu_1 - \mu_7) & 1 + \mu_8 - \left(\frac{4\theta}{\Omega}\right)^2 \\ -(\mu_4 - \mu_6) & -(\mu_3 - \mu_7) & -(\mu_2 - \mu_8) & -(\mu_1 - \mu_9) \end{vmatrix} = 0 \dots (8)$$

$$\begin{vmatrix} 1 & -\mu_1 & -\mu_2 & \mu_3 \\ -2\mu_1 & 1 - \mu_2 - \left(\frac{\theta}{\Omega}\right)^2 & -(\mu_1 + \mu_3) & -(\mu_2 + \mu_4) \\ -2\mu_2 & -(\mu_1 + \mu_3) & 1 - \mu_4 - \left(\frac{2\theta}{\Omega}\right)^2 & -(\mu_1 + \mu_5) \\ -2\mu_3 & -(\mu_2 - \mu_4) & -(\mu_1 + \mu_5) & 1 - \mu_6 - \left(\frac{3\theta}{\Omega}\right)^2 \\ -1\mu_4 & -(\mu_3 + \mu_5) & -(\mu_2 + \mu_6) & -\left(\mu_1 + \mu_7\right) \end{vmatrix} = 0 \dots (9)$$

RESULTS AND DISCUSSION

By writing the periodic rectangular and triangular force, as shown in figure 2, respectively:

$$p(t) = p_o + p_1 \left(\cos \theta t - \frac{1}{3} \cos 3\theta t + \frac{1}{5} \cos 5\theta t \dots \right) \dots \dots (10)$$

$$p(t) = p_o + p_1 \left(\cos \theta t - \frac{1}{5} \cos 3\theta t + \frac{1}{25} \cos 5\theta t \dots \right) \dots \dots (11)$$

The primary and secondary instability limits zones of the first mode for both sides simply supported column are calculated by the computer (use MATLAB program). This was done by solving the matrix of the three equations (7, 8 and 9). Figure 3, explains the instability zones of the three periodic forces. From this figure, it can be noted that the primary zone limit doesn't affect even at the high values of the excitation parameter while the zone get off by the sinusoidal periodic force for the same excitation parameter. Also, at $(5.\mu_1=0.5)$, the increasing or reduction in the secondary instability zone-wide about (+27%, -9%) when applying rectangular or triangular periodic force comparing with sinusoidal periodic force.

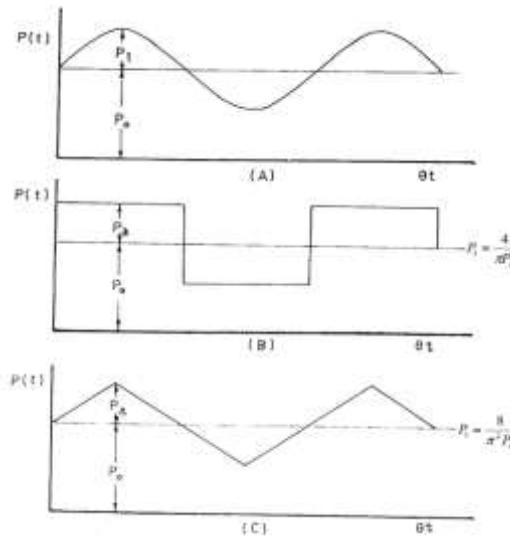


Figure 2. Different types of periodic axial force A: sinusoidal, B: Rectangular, C: triangular

In equation (7), which controls the primary instability zone, the solving of matrix (2 x 2) gives a result within $\pm 5\%$ from this that calculated with high grade matrix even at high values of the excitation parameter. In another word, the absent of (μ_2) from the Fourier series of the rectangular, triangular periodic force and small equations that are related to (μ_5, μ_3) , led to a slight difference in calculated values between the sinusoidal, rectangular and trigonometric forces. In another side, the effect of (μ_3) is clear when solving matrix with a third or second grade to obtain the secondary instability zone limit. The sign of (μ_3) refer to the increasing or reducing the zone area. In addition, (μ_4, μ_5, \dots) had similar effects but in a very small values due to the their position in the matrix. Moreover, the addition of the secondary force, $P_2 \cos 2\theta t$, to the primary dynamic force, $P_0 + P_1 \cos \theta t$, had an obvious effect on primary instability zones. Where, it will be moved up to the upper limit leading to a decrease in the area of this dangerous area.

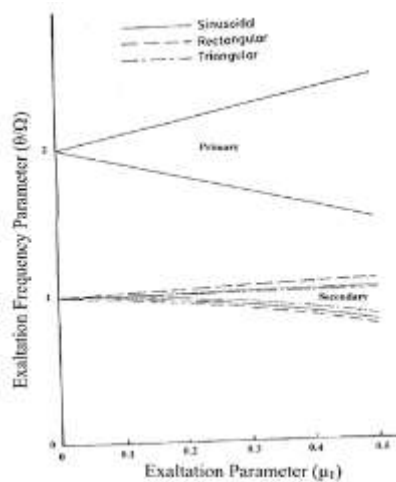


Figure 3. Region of parameter instability belongs to three types of axial loading

A significant effect was also observed on the boundaries of the secondary instability zone, where, with increasing (μ_2), the area increased sharply, Figure 4. This phenomenon is due to the fact that the frequency (θ) of the dependent (P1), there are areas of primary instability primary, secondary and third etc. with decreasing areas of one relative to the other. Similarly, there are regions similar to the frequency (2θ) of the force (P2), as the secondary region generated by the frequency (2θ) is identical to the secondary region generated by the frequency (θ), causing this phenomenon. The resulting region is not the algebraic sum of the two regions, but their sum will be according to the determinants, [9, 8]. A small effect of high values of (μ_3) was observed on the boundaries of the region for the initial instability, as shown in Figure 5, while a clear decrease of the area occurred in the secondary zone.

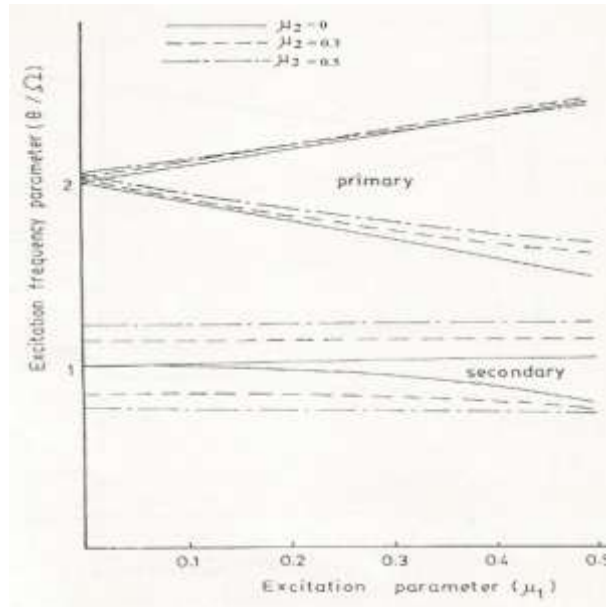


Figure 4. Effect of added (μ_2) on regions of instability

The boundaries of this region intersect at a displacement point to the right causing two instability regions to occur. From the value ($\mu_1 = 0$) to the intersection point, the lower bound becomes top and vice versa. The boundaries of the secondary instability zone were shifted slightly when adding a secondary force ($P_4 \cos 4\theta t$) to the primary dynamic force ($P_0 + P_1 \cos \theta t$). Also, no effect of this force was observed on the boundaries of the primary region. The engineering view of the $P_6 \cos 6\theta t$, $P_5 \cos 5\theta t$ forces has no influence on the boundaries of the primary and secondary instability regions, figure 6.

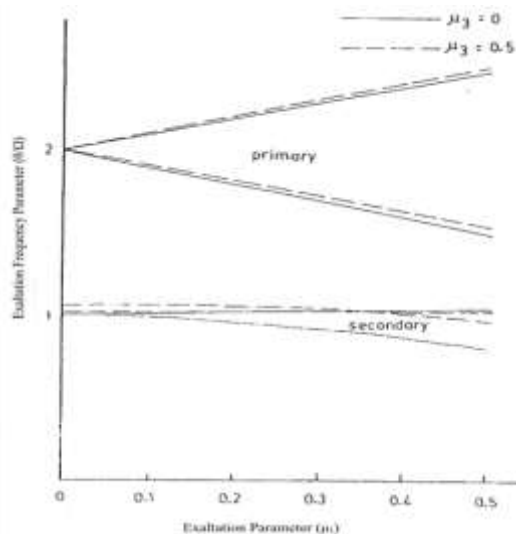


Figure 5. Effect of added (μ_3) on regions of instability

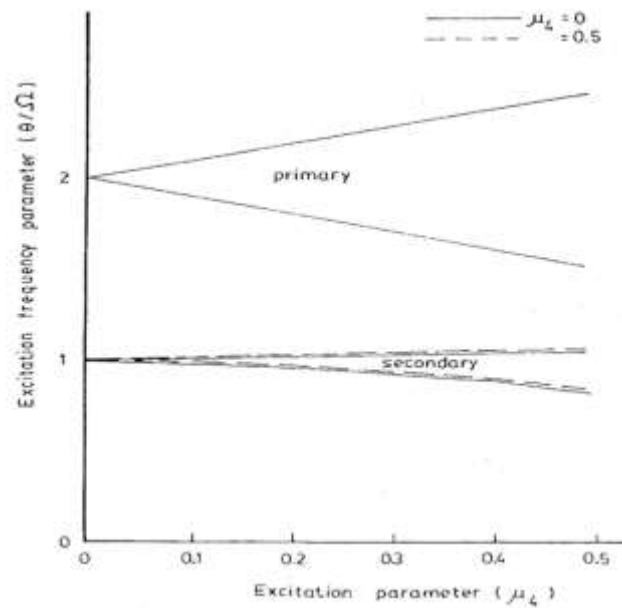


Figure 6. Effect of added (μ_4) on regions of instability

CONCLUSIONS

Through the parametric stability of the flexible columns under the influence of different types of axial dynamic periodic loading, the results are as follows:

1. The boundaries of the initial instability zone were the same for the three periodic forces (sinusoidal, rectangular, and trigonometric). As for the secondary instability zone, their area increases or decreases according to the type of loading.
2. With increasing the added value of the (μ_2), the secondary instability zone expands and the lower border of the primary region shifts to the top.
3. A slight effect on the primary region boundaries is observed when adding an impact force of type ($P_4\cos 40t$, $P_3\cos 30t$) and a clear decrease in the area of the secondary area when adding the $P_3\cos 30t$ force.
4. There were no tangible effects on the boundaries of the instability areas when adding ($P_6 \cos 60t$, $P_5 \cos 50t$ etc.) to the initial dynamic force ($P_0 + P_1 \cos 0t$).

REFERENCES

- [1] B.L. Rhode, Jain, H.P. Kripakaran and I.F. Smith, "Design of tensegrity structures using parametric analysis and stochastic search" *Engineering with Computers*, Vol. 26, No. 2, Pp 193-203, 2010.
- [2] G. Mikhail, D. Aleksandr, D. Arcady and P. Elena P., "Dynamic stability of rolling particles between elastic plates", Vol. 19, EGU2017-3867, 2017, EGU General Assembly 2017, © Author(s) 2017. CC Attribution 3.0 License.
- [3] B. Kang, T. Carissa, "Parametric instability of a Leipholz column under periodic excitation", *Journal of Sound and Vibration*, Vol. 229, No. 5, Pp. 1097-1113, 2000.
- [4] H. Youqin, L. Airong, P. Yonglin, L. Hanwen, W. Gao, "Assessment of lateral dynamic instability of columns under an arbitrary periodic axial load owing to parametric resonance)", *Journal of Sound and Vibration*, 2017. journal home page: www.elsevier.com/locate/jsvi, <http://dx.doi.org/10.1016/j.jsv.2017.02.031i>,
- [5] P.R. Dash, M. Pradhan, A. Bisoi, "Parametric instability of an asymmetric sandwich beam with thermal gradient under various boundary conditions by computational method", *Elsevier/ Procedia Engineering*, 144, Pp. 900 – 907, 2016.

- [6] T.H. Mohamed, A.H. Samir, "Analysis of Nonuniform Beams on Elastic Foundations Using Recursive Differentiation Method", *Engineering Mechanics*, Vol. 22, No. 2, Pp. 83–94, 2015.
- [7] G. Oliver, and J. Darío, "Dynamic stability of slender columns with semi-rigid connections under periodic axial load", *DYNA*, 81 (185), Pp. 56-65, 2014.
- [8] I. Ramu, "On the Dynamic Stability of Functionally Graded Material Plates Under Parametric Excitation", PhD theses, Department of Mechanical Engineering, National Institute of Technology, Rourkela -769008 Odisha (India), June-2015.
- [9] P. Ratko, and R. Ivan, "Dynamic Stability of Timoshenko Beams on Pasternak Viscoelastic Foundation", *Theoretical And Applied Mechanics*, Vol. 45, No. 1, Pp. 67–81, 2018.
- [10] A.A. Mailybaev, and A.P. Seyranian, "Stabilization of statically instability columns by axial vibration of arbitrary frequency", *Journal of Sound and Vibration*, 328, Pp. 203–212, 2009.
- [11] P. Fritzkowski, " Transverse vibrations of a beam under an axial load minimal model of a triangular frame", Springer, Applied Mechanics, DOI 10.1007/s00419-016-1156-2, 20 June 2016.